ISSN 0021-3640, JETP Letters, 2024, Vol. 119, No. 1, pp. 27–33. © The Author(s), 2024. This article is an open access publication.
Russian Text © The Author(s), 2024, published in Pis'ma v Zhurnal Eksperimental'noi i Teoreticheskoi Fiziki, 2024, Vol. 119, No. 1, pp. 27–33.

PLASMA, HYDRO- AND GAS DYNAMICS

Features of the Dynamic Spectrum of Signals Generated by a Wide-Aperture Electron Beam in a Large-Scale Magnetized Plasma

I. Yu. Zudin[a,*], M. E. Gushchin[a], A. V. Strikovskiy[a], N. A. Aidakina[a], S. V. Korobkov[a], A. S. Nikolenko[a], V. I. Gundorin[a†], K. N. Loskutov[a], and A. G. Demekhov[a]

[a] *Institute of Applied Physics, Russian Academy of Sciences, Nizhny Novgorod, 603950 Russia*

**e-mail: zudiniy@ipfran.ru*

Received November 8, 2023; revised November 17, 2023; accepted November 20, 2023

Electromagnetic signals generated by a wide-aperture electron beam in the laboratory plasma under conditions limitedly modeling the interaction between waves and particles in the near-Earth plasma have been studied at the large-scale Krot device. The spectrum of electromagnetic radiation includes whistler noise, which is presumably due to the current instability, and discrete (narrowband) signals near harmonics of the electron cyclotron and plasma frequencies. It has been shown that narrowband signals with a positive frequency drift that are observed at the injection of the electron beam are caused by nonstationary variations of the plasma density due to an additional ionization of a neutral gas by accelerated electrons. These effects should be taken into account to interpret nonconventional forms of the dynamic spectrum in various laboratory experiments simulating processes in the Earth's ionosphere and magnetosphere.

DOI: 10.1134/S0021364023603524

The generation of electromagnetic radiation by high-energy electron beams is a phenomenon well known in the space plasma; attempts of its laboratory simulation continued during almost five decades [1]. Laboratory simulation is considered as a promising approach that supplements nature studies and allows the qualitative understanding of the nature of developed plasma instabilities, as well as the verification of theoretical and numerical models using similarity criteria [2].

A significant part of types of radiation in the near-Earth plasma (chorus, hiss, triggered emission, whistling sferics, etc.) are generated in the form of whistler waves with frequencies satisfying the condition $f_{lh} < f < f_{ce} < f_p$, where f_{lh}, f_{ce}, and f_p are the frequencies of low-hybrid, electron cyclotron, and plasma resonances, respectively [3]. The generation of whistler waves by electron beams is also actively studied in the laboratory plasma. It was previously found in laboratory experiments that "narrow" monoenergetic electron beams with the width smaller than $\delta_e = c/(2\pi f_p)$ (where c is the speed of light in vacuum) in the background magnetized plasma are stable and emit whistler waves only in the presence of the initial modulation [4]. Laboratory experiments with a "wide" spatial distribution of electrons having the energy distribution function with a "tail," where the generation of electromagnetic signals due to the development of certain instabilities is observed are closer to the natural situation. Radiation bursts with a complex spectrum similar to magnetospheric chorus emissions [5, 6] are observed in the nonequilibrium plasma of the electron-cyclotron resonance discharge [7, 8] and at the injection of wide electron beams into the laboratory plasma [9, 10]. In addition to whistler waves, signals at frequencies of ion and electron gyroharmonics are quite widespread [11–13]. The theory predicts that such signals are generated most efficiently under the conditions of double plasma resonance [14], which was also observed in laboratory experiments [15].

In [16], we described the current instability induced by an electrode under a high positive voltage in the magnetized plasma column, which is accompanied by the generation of a wide spectrum of whistler waves. It is remarkable that, although the beam of accelerated particles was formed by their extraction from the background magnetized plasma and energies and velocities were comparatively low, the general picture of generation of whistler waves and some features of their spectrum, including a dip near half the gyrofrequency, were similar to the results that were previously obtained with wide-aperture electron beams and were attributed to the development of kinetic instabil-

† Deceased.

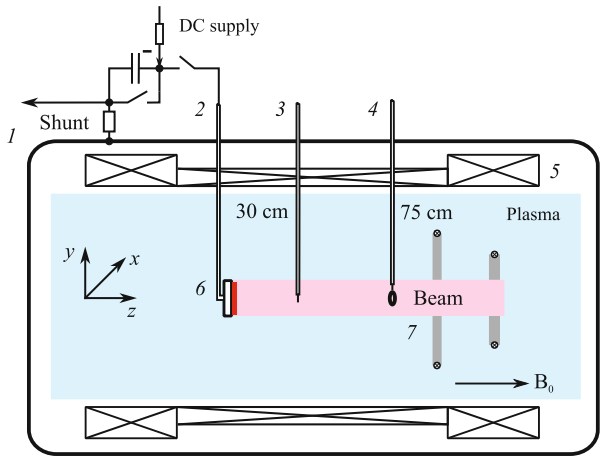

Fig. 1. (Color online) Schematic diagram of the plasma device: (*1*) vacuum chamber, (*2*) high-voltage source, (*3*) Langmuir probe, (*4*) loop antenna or microwave resonator probe, (*5*) solenoid, (*6*) hot cathode, and (*7*) inductors for plasma generation.

ities to explain magnetospheric effects [10]. For this reason, to better understand the possible nature of observed signals, we carried out a new experiment on the injection of the wide-aperture electron beam into a large magnetized plasma column with the plasma parameters close to both those used in [16] and the parameters of the setup in [9, 10].

Figure 1 presents the schematic diagram of the Krot plasma device [17], where the experiment was carried out. The plasma was induced by a pulsed inductive discharge in argon at a pressure of $p_0 = 4\times10^{-4}$ Torr in a magnetic field up to 1 kG. The maximum plasma density at the source operation was about 2×10^{12} cm^{-3} and the electron temperature was $T_e \sim 5$ eV. The device operated in the pulse-periodic regime with a pulse repetition interval of 20 s. Experiments were conducted after the end of the ionizing pulse in a quite decaying plasma with the characteristic diffusion decay time of several milliseconds. In the process of decay, electrons were cooled to $T_e \sim 0.5$ eV in a time of about 1 ms, and the ion temperature was $T_i \approx T_e$. A high (within 1%) reproducibility of the plasma parameters in all "shoots" of the plasma device allowed multiply repeated measurements, collecting a huge body of experimental data.

The wide-aperture electron beam was produced by the hot cathode, which had the form of a flat tungsten spiral coated by lanthanum hexaboride and having a pitch of 5 mm and a diameter of 80 mm. Electrons were accelerated by a pulsed voltage with a duration of 50–120 μs, a magnitude of $U_b = 30$–300 V, and a negative polarity with respect to the chamber wall applied to the cathode; the total emission current of the cathode reached 1.5 A. The hot cathode was mounted on a sliding rod with a vacuum seal; in all experiments, the cathode was placed on the axis of the plasma column with the spiral plane perpendicular to the magnetic field.

The electron beam was injected into either the background plasma ($N_e \approx 10^{11}$ cm^{-3}, $f_p \approx 2.85$ GHz, $T_e \approx 0.5$ eV) or neutral argon gas at a pressure of $p_0 = 4\times10^{-4}$ Torr. The static magnetic field varied in the range $B_0 = 40$–180 G ($f_{ce} = 110$–500 MHz). The temperature and plasma density were measured by the Langmuir probe; the plasma density was also independently measured by a microwave-resonator probe on a section of a double line [18]. The ac magnetic field of signals generated by the electron beam was measured by a single-loop antenna 1 cm in diameter, which was placed in an electrostatic shield and was isolated from the plasma by a dielectric layer. The probes and antenna mounted on rods could freely move across the plasma column.

The waveforms were recorded by Tektronix MDO 4054-3 (500-MHz band) and Tektronix MSO 54 (2-GHz band) digital oscilloscopes; spectral characteristics in their dynamics were determined by the digital processing of waveforms using the window Fourier transform method. It is important that the incorrect application of modern broadband digital oscilloscopes can provide false signals and erroneous results, in particular, in the laboratory simulations of magnetospheric emissions (see, e.g., [19] and the subsequent correction in [20]). For this reason, when analyzing signals whose spectrum is not known a priori in detail, great attention was paid to the control of the spectral composition of waveforms under processing in an extended frequency band and to their anti-aliasing filtering, as well as to the control of processing procedures on simulated (test) waveforms.

Figure 2a presents the electron density and the parameters of the electron distribution function measured at the injection of the electron beam into the magnetized background plasma. Here and below, the results of the experiment are presented in the Cartesian coordinate system that is associated with the cathode and is shown in Fig. 1: the z axis is directed along the chamber axis and the magnetic field, whereas the x and y axes are horizontal and vertical, respectively. Before the application of an accelerating voltage pulse, a depleted density region or "shadow" existed on the cathode due to losses of particles of the background plasma. After the beginning of injection, an additional ionization of neutral gas and the heating of the plasma with the formation of a two-temperature distribution function ($T_{e1} \approx 2$ eV and $T_{e2} \approx 5$ eV) occurred in a magnetic tube based on the cathode. Due to the additional ionization, the electron density N_e on the axis of the electron beam after about 100 μs was even higher than the background value.

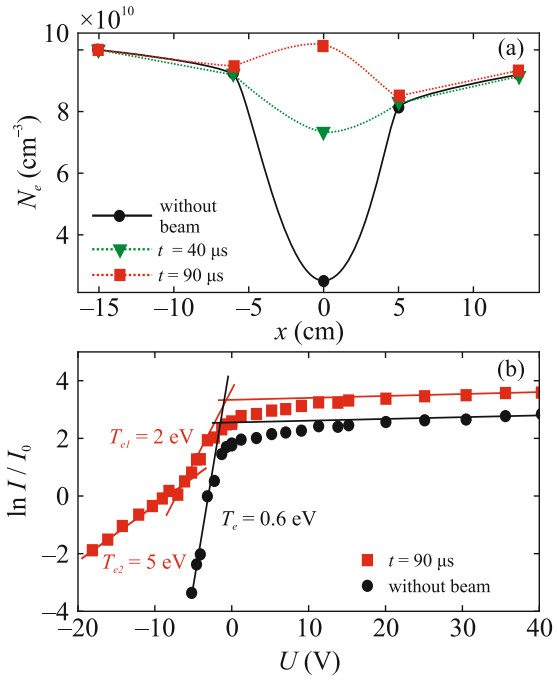

Fig. 2. (Color online) (a) Distribution of the plasma density and electron temperature in the cross section of the plasma column at the injection of electrons. (b) Current–voltage characteristic of the Langmuir probe obtained on the axis of the electron beam at $B_0 = 90$ G and $U_b = 125$ V.

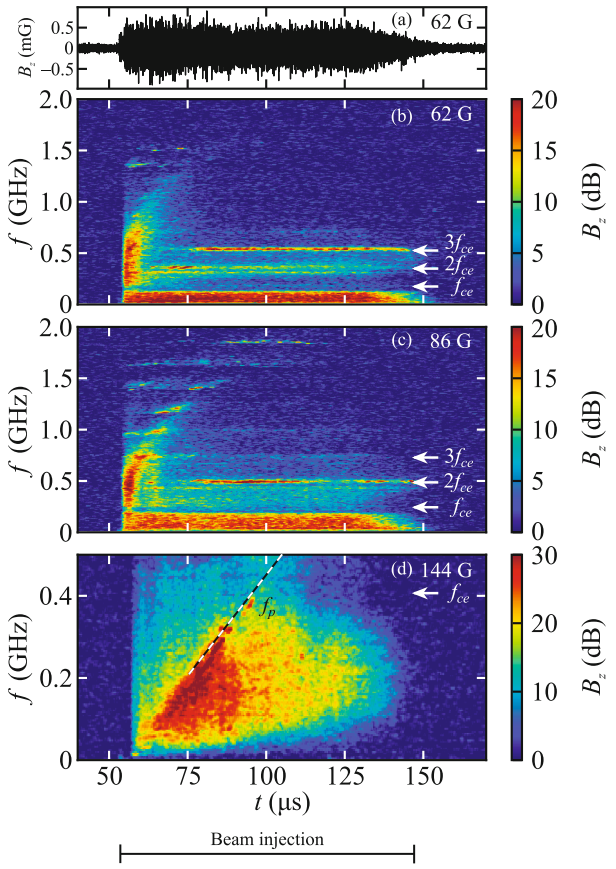

Fig. 3. (Color online) Electromagnetic noise detected at an accelerating voltage of $U_b = 250$ V. (a) Waveform of noise in the frequency range of 10–750 MHz (injection into the background plasma at $B_0 = 62$ G and $f_{ce} = 174$ MHz). (b–d) Spectrograms of noise (b, c) at injection into the background plasma at (b) $B_0 = 62$ G and $f_{ce} = 174$ MHz and (c) $B_0 = 86$ G and $f_{ce} = 243$ MHz and (d) at injection into neutral argon at $B_0 = 144$ G and $f_{ce} = 404$ MHz; the dashed line is the plasma frequency. Gyroharmonics are marked by arrows.

When electrons were injected into the neutral gas, the plasma was induced only in the magnetic tube based on the cathode and had the form of a thin plasma column 5 cm in diameter with the maximum electron density $N_e \approx 10^{11}$ cm^{-3}. In this case, the two-temperature distribution function of electrons was also formed, but the temperatures of both populations ($T_{e1} \approx 6$ eV and $T_{e2} \approx 17$ eV) were about three times higher than those in the case of injection into the plasma probably due to lower losses on heat conductivity in the background medium.

Intense electromagnetic noise was generated at the injection of electrons into both the plasma and neutral gas (Fig. 3a). The typical amplitude of noise in the frequency band 10–750 MHz is 100–500 μG and the peak amplitude is about 1 mG. Dynamical spectra (frequency–time spectrograms) of noise are shown in Figs. 3b–3d. All spectrograms were normalized to the amplitude of the noise spectrum before the beginning of injection.

If the plasma in the beginning of the injection of electrons was absent or its density satisfied the condition $f_p < f_{ce}$ (rare plasma case), the noise amplitude at any time is maximal near f_p. A "plasma line" $f \approx f_p(t)$ analogous to the time dependence of the electron density N_e before the condition $f_p \approx f_{ce}$ was formed on the dynamic spectrum (see Fig. 3d). If electrons were injected into the background plasma under the condition $f_p > f_{ce}$ (dense plasma case), pronounced dynamic spectral components with increasing frequencies, which are similar to the plasma line, are also present in the initial stage (see Figs. 3b and 3c).

Spectrograms of signals with frequency drift in the dense plasma are shown in more detail in Fig. 4. The frequency of some spectral elements increases at a rate of about 10 MHz/μs; the duration of such elements varies in the range of 3–10 μs. Bursts appear with the time at increasing frequencies, and the general behavior of the dynamic spectrum approximately corresponds to the evolution of the electron density $N_e(t)$ in the magnetic tube based on the cathode. According to probe measurement data presented in Fig. 2a, the plasma frequency f_p during the first 50 μs of the injection of electrons increased from 1 to 2 GHz, which

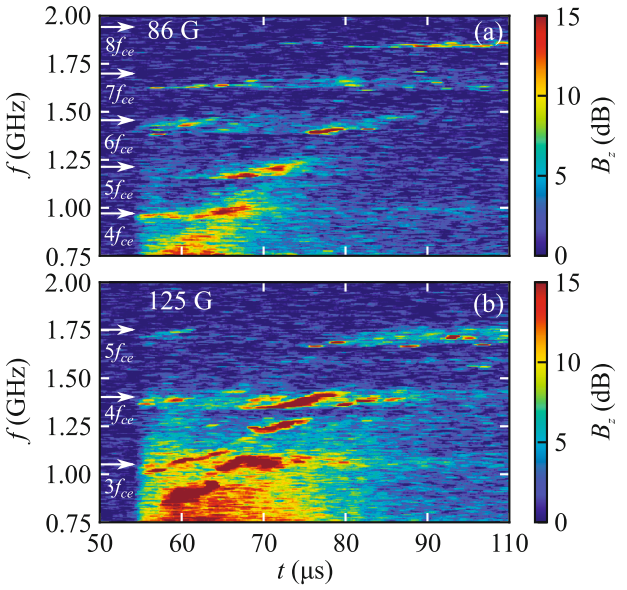

Fig. 4. (Color online) Fine dynamic structure of the spectrum of signals in the beginning of electron injection into the background plasma at (a) B_0 = 86 G and f_{ce} = 243 MHz and (b) B_0 = 125 G and f_{ce} = 350 MHz. Gyroharmonics are marked by arrows.

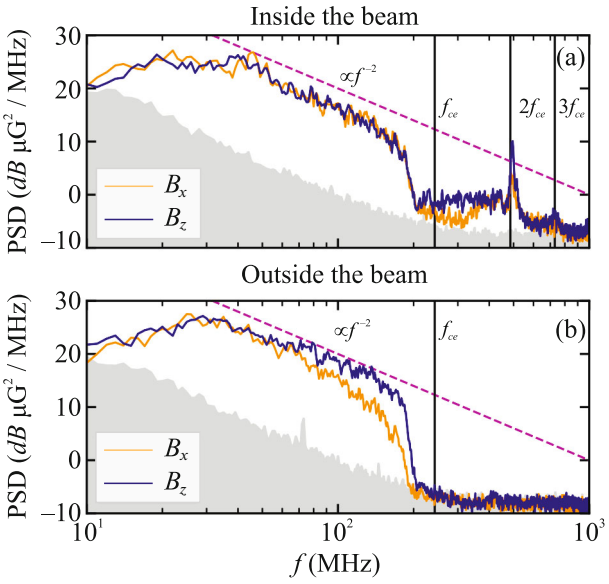

Fig. 5. (Color online) Spectra of the longitudinal (B_z) and transverse (B_x) components of magnetic noise in experiments (a) inside and (b) outside the electron beam in the time interval 45–65 μs after the beginning of injection at B_0 = 86 G and f_{ce} = 243 MHz. The noise of the system is shown in gray, the black vertical straight lines mark the first and second harmonics of the electron gyrofrequency, and the dashed line is PSD $\propto f^{-2}$.

corresponds to the general behavior of the intensity of bursts in a frequency–time domain.

In about 50 μs after the beginning of the injection of electrons into the gas or the plasma, the electron density N_e was established at a quasistationary level corresponding to the dense plasma case $f_p > (\gg) f_{ce}$. In this case, a continuous noise spectrum weakened near the gyrofrequency f_{ce} was detected (see Figs. 3b and 3c). Above f_{ce}, in the plasma evanescence band to electromagnetic radiation, narrowband signals with frequencies close to the gyroharmonics $2f_{ce}$, $3f_{ce}$, $4f_{ce}$, etc. were certainly detected inside the electron beam.

Time-averaged frequency spectra of the longitudinal (B_z) and transverse (B_x) components of magnetic noise inside the electron beam and at its periphery are shown in Fig. 5. The components B_z and B_x inside the electron beam are comparable, and their power spectrum decreases by a law close to $\propto f^{-2}$. At frequencies $f > f_{ce}$ inside the electron beam in the source region, broadband noise is also present but its level is lower than that in signals at gyroharmonics nf_{ce}. The spectrum outside the electron beam has a sharp edge $f \approx f_{ce}$: noise consists of whistler waves emitted into the ambient plasma.

Let us now discuss in more detail various spectral component of electromagnetic signals.

Noise of the continuous spectrum is close in properties to the whistler instability at the extraction of electrons from the plasma to the electrode [16]. First, the nonequilibrium (unstable) character of noise is confirmed by the fact that its level is two orders of magnitude higher than the estimated thermal noise on the loop antenna in the plasma [21] even at the maximum electron temperature T_e = 5 eV (see Fig. 2) and at the estimate of the resistance of antenna radiation increased to R_{rad} = 0.5 Ω. After the end of electron injection, noise at the trailing edge of the accelerating voltage pulse disappeared in a time no longer than 10 μs, which is one or two orders of magnitude smaller than the relaxation time of the electron temperature T_e.

Second, the geometry of the electric current induced at the injection of electrons into the magnetized plasma mainly repeats the current structure at the extraction of electrons from the plasma on the high-voltage electrode [16]. The accelerating voltage is applied directly between the cathode and the grounded wall of the vacuum chamber, but the current–voltage characteristic of the Langmuir probe (Fig. 2) shows that the plasma potential at a distance of ~30 cm from the cathode does not change at the application of the accelerating voltage. This indirectly indicates that the entire voltage drop occurs in the near-cathode region: the background plasma carries the potential of the chamber wall to the region $z <$ 30 cm due to its high conductivity. The maximum gyroradius of electrons accelerated near the cathode

corresponding to an energy of 300 eV and $B_0 \sim 50$ G is $\rho_e \approx 1$ cm; the gyroradii of electrons with $T_e = 2$–5 eV do not exceed 1 mm. The mean free path of electrons determined by Coulomb collisions is $l_e > 1$ m in the entire energy range. Thus, electrons accelerated in the near-cathode regions are strongly magnetized, and their gyroradii are much smaller than the sizes of the cathode. Since the transverse sizes of the background plasma are much larger than both the diameter of the cathode and the magnetic tube filled with accelerated electrons, the electric circuit can be closed only by the parallel electron current flowing in the plasma along the z axis. This geometry reproduces that described in [16] with the accuracy to the direction of electron motion: electrons in [16] moved from the plasma toward the collecting electrode (collector), whereas in this work, they move from the emitting electrode (hot cathode) to the plasma.

Third, the spectral properties of noise correspond to the picture from [16]: signals have a continuous spectrum with the upper edge at the frequency f_{ce} outside the generation region. The noise amplitudes in this work are also consistent with those in [16]. The developed instability at the total current $I \sim 100$ A of electrons extracted from the plasma and its density $j_z \sim 1$ A/cm^2 led in [16] to the generation of noise with a peak amplitude of about 10 mG and a standard deviation of 0.1–1 mG. In this work, the total current of emitted electrons passing through the area of the same cross section is about two orders of magnitude lower and the noise amplitude at similar plasma parameters and the frequency band is smaller by a factor of 10–30. Since electrical circuits are incompletely equivalent and details of the spatial structure and the evolution of the current are different, this agreement should be considered as good and, moreover, as indicating the closeness of mechanisms of noise generation with the continuous frequency spectrum due to the development of the current instability both at the extraction of electrons from the plasma and at their emission into the plasma.

Whistler noise with the continuous spectrum is characteristic of a number of beam–plasma experiments simulating the generation of electromagnetic emissions in the Earth's ionosphere and magnetosphere [1, 9, 10]. The results obtained in [16] and in this work indicate that the mechanism of generation of whistler noise in systems with the parallel current is common for fast monoenergetic electron beams [9, 10] and for electron beams with a moderate velocity and a high energy spread.

Signals at electron gyroharmonics are also quite typical of beam–plasma systems. These signals are usually not caused by the excitation of any eigenmodes of the plasma (e.g., quasielectrostatic electron cyclotron waves) but are due to the interference of the fields of electrons moving along spiral trajectories and are detected by magnetic antennas only inside the electron beam [21, 22]. Outside the electron beam, radiation at gyroharmonics is absent. This distinguishes the laboratory experiment from space observations [13] mentioned in the beginning of this work, where signals at gyroharmonics detected by electrical antennas are explained by the instability of Bernstein modes (electron or ion), in particular, under the conditions of double plasma resonance.

The generation of narrowband bursts with frequency drift is of particular interest for the simulation of physical phenomena in the near-Earth plasma. Some authors consider the appearance of signal with frequency drift either positive (increasing tone) or negative (decreasing tone) as evidence of the similarity of the laboratory experiment to the space observation [23]. At the same time, when nonstationary variations of the electron density $N_e(t)$, which are due either to an additional ionization of the neutral gas by injected electrons or to the decay of the plasma, are taken into account, the appearance of signals with the frequency drift in the band corresponding to the range of variation of the electron plasma frequency $f_p(t)$ is less surprising. In particular, measurements of the time dependence of the frequency of the spectral line excited near f_p by the low-current electron beam injected into the plasma are used for the precise diagnostics of the density of the decaying plasma [24]. In our experiment, the generation of increasing narrowband tones can be caused by mechanisms characteristic of a nonstationary beam–plasma discharge accompanied by the excitation of quasi-electrostatic (Langmuir) waves and signals at electron gyroharmonics [25]. Obviously, the complete explanation of the fine structure of the spectrum presented in Fig. 4 is impossible in this stage but the relation of this structure to the increase in the plasma density accompanied by the dynamical variation of the electron plasma frequency and dispersion properties of the plasma as a whole is certainly seen.

To explain the effects of generation of noise-like and discrete radiation bursts in some beam–plasma experiments on the laboratory simulation of space phenomena, the same mechanisms of interaction between electrons and waves in cyclotron resonance applied to interpret space phenomena are used [10, 23]. However, the cited studies are usually performed in a low-temperature argon plasma, which has the same parameters as in the Krot device, including the electron density and the pressure of the neutral gas, magnetic field strength, and the scale of the interaction region of electrons with the background medium. Despite obvious manifestations of the interaction of electrons with the neutral gas such as bright optical emission [23], the possible effect of the additional ionization of the neutral gas or the plasma decay on signals generated by the electron beam was not discussed in the cited works. Narrowband whistler signals with decreasing frequency reported in [23] have a duration

of about 1 ms, which corresponds to the characteristic time of variations of the plasma parameters possible in such an experiment. For this reason, we believe that the radiation frequency drift shown in [23] can be naturally attributed to the nonstationarity of the medium rather than to the nonlinear wave–particle interaction.

The results obtained in this work can be briefly summarized as follows. The current instability responsible for the generation of broadband whistler signals is fairly universal; it is observed both at the injection of accelerated electrons (with a monoenergetic or broad spectrum) into the plasma and at the extraction of electrons from the plasma by the parallel electric field. Such an instability observed in various laboratory devices should also be manifested in the near-Earth plasma including the auroral ionosphere. Furthermore, electrons injected into the magnetized plasma generate narrowband signals at electron gyroharmonics and at frequencies close to the local electron plasma frequency. In the latter case, the pulsed injection can result in the generation of signals with frequency drift caused by the plasma dynamics due to the additional ionization of the neutral gas. The additional ionization can qualitatively change the conditions for the generation of electromagnetic radiation due to a change in the relations between resonance frequencies of the plasma and create favorable conditions for the ducted propagation of waves [26], which promotes an increase in the efficiency of wave–particle interactions in the near-Earth plasma, including active experiments. All these effects should be taken into account when planning experiments in the ionosphere, in particular with the injection of pulsed electron beams from spacecrafts, and interpreting their results.

To conclude, we note a high significance of the laboratory simulation results obtained in [9, 10, 23] and in other works that provide valuable experimental data, which can be used to propose new and to develop existing models of the interaction between waves and particles in the ionosphere and magnetosphere. The reported experiment does not reproduce in detail the cited beam–plasma studies, primarily in the energies of electrons, which are several keV in those works, and in the quality of the electron beam. However, it is obvious that conclusions on the similarity of the generation of radiation bursts with a complex spectrum in the laboratory and space should be made carefully without the complete diagnostic information on the plasma and the critical analysis of all features of the laboratory experiment, including additional factors such as the considered additional nonstationary ionization of the neutral gas.

ACKNOWLEDGMENTS

The experiments were carried out using the unique scientific setup "Complex of Large-Scale Geophysical Facilities" at the Institute of Applied Physics, Russian Academy of Sciences.

FUNDING

This work was supported by the Ministry of Science and Higher Education of the Russian Federation (state assignment no. FFUF-2021-0028 for the Institute of Applied Physics, Russian Academy of Sciences; experimental studies and result processing). M.E. Gushchin and A.G. Demekhov acknowledge the support of the Russian Science Foundation (project no. 21-12-00385, analysis of the results in application to the simulation of the interaction between waves and particles in the near-Earth plasma).

CONFLICT OF INTEREST

The authors of this work declare that they have no conflicts of interest.

OPEN ACCESS

This article is licensed under a Creative Commons Attribution 4.0 International License, which permits use, sharing, adaptation, distribution and reproduction in any medium or format, as long as you give appropriate credit to the original author(s) and the source, provide a link to the Creative Commons license, and indicate if changes were made. The images or other third party material in this article are included in the article's Creative Commons license, unless indicated otherwise in a credit line to the material. If material is not included in the article's Creative Commons license and your intended use is not permitted by statutory regulation or exceeds the permitted use, you will need to obtain permission directly from the copyright holder. To view a copy of this license, visit http://creativecommons.org/licenses/by/4.0/

REFERENCES

1. R. L. Stenzel, J. Geophys. Res. **82**, 4805 (1977).
2. H. Alfven and G. G. Felthammar, *Cosmical Electrodynamics* (Clarendon, Oxford, 1963).
3. R. A. Helliwell, *Whistlers and Related Ionospheric Phenomena* (Stanford Univ. Press, CA, 1965).
4. M. Starodubtsev, and C. Krafft, Phys. Rev. Lett. **83**, 1335 (1999).
5. W. J. Burtis and R. A. Helliwell, Phys. Status Solidi **24**, 1007 (1976).
6. X.-J. Zhang, A. G. Demekhov, Y. Katoh, D. Nunn, X. Tao, D. Mourenas, Y. Omura, A. V. Artemyev, and V. Angelopoulos, J. Geophys. Res. Space Phys. **126**, e2021JA029330 (2021).
7. A. G. Shalashov, A. V. Vodopyanov, S. V. Golubev, A. G. Demekhov, V. G. Zorin, D. A. Mansfeld, and S. V. Razin, JETP Lett. **84**, 314 (2006).
8. M. E. Viktorov, A. G. Shalashov, E. D. Gospodchikov, N. Yu. Semin, and S. V. Golubev, Phys. Plasmas **27**, 062104 (2020).

9. X. An, B. van Compernolle, J. Bortnik, R. M. Thorne, L. Chen, and W. Li, Geophys. Res. Lett. **43**, 2413 (2016).
10. B. van Compernolle, X. An, J. Bortnik, R. M. Thorne, P. Priby, and W. Gekelman, Plasma Phys. Control. Fusion **59**, 014016 (2017).
11. S. N. Walker, A. G. Demekhov, S. A. Boardsen, N. Y. Ganushkina, D. G. Sibeck, and M. A. Balikhin, J. Geophys. Res. Space Phys. **121**, 9701 (2016).
12. N. P. Meredith, R. B. Horne, R. M. Thorne, and R. R. Anderson, J. Geophys. Res. **114**, A07218 (2009).
13. R. M. Thorne, B. Ni, X. Tao, R. B. Horne, and N. P. Meredith, Nature (London, U.K.) **467**, 943 (2010).
14. V. V. Zheleznyakov and E. Y. Zlotnik, Solar Phys. **44**, 461 (1975).
15. M. E. Viktorov, S. V. Golubev, V. V. Zaitsev, and D. A. Mansfeld, Radiophys. Quantum Electron. **57**, 849 (2014).
16. I. Yu. Zudin, M. E. Gushchin, N. A. Aidakina, S. V. Korobkov, and A. V. Strikovskiy, JETP Lett. **113**, 86 (2021).
17. N. A. Aidakina, A. G. Galka, V. I. Gundorin, M. E. Gushchin, I. Yu. Zudin, S. V. Korobkov, A. V. Kostrov, K. N. Loskutov, M. M. Mogilevskiy, S. E. Priver, A. V. Strikovskiy, D. V. Chugunin, and D. V. Yanin, Geomagn. Aeron. **58**, 314 (2018).
18. R. L. Stenzel, Rev. Sci. Instrum. **47**, 603 (1976).
19. B. Van Compernolle, X. An, J. Bortnik, R. M. Thorne, P. Pribyl, and W. Gekelman, Phys. Rev. Lett. **114**, 245002 (2015).
20. B. Van Compernolle, X. An, J. Bortnik, R. M. Thorne, P. Pribyl, and W. Gekelman, Phys. Rev. Lett. **117**, 059901 (2016).
21. G. Golubyatnikov and R. L. Stenzel, Phys. Fluids B **5**, 3122 (1993).
22. R. L. Stenzel and G. Golubyatnikov, Phys. Fluids B **5**, 3789 (1993).
23. E. M. Tejero, C. Crabtree, D. D. Blackwell, W. E. Amatucci, G. Ganguli, and L. Rudakov, Phys. Plasmas **23**, 055707 (2016).
24. R. L. Stenzel, Phys. Fluids B **1**, 1369 (1989).
25. E. G. Shustin, Plasma Phys. Rep. **47**, 536 (2021).
26. Yu. N. Agafonov, V. S. Bazhanov, V. Ya. Isyakaev, G. A. Markov, A. A. Pokhunkov, Yu. V. Chugunov, and S. A. Kulistikov, JETP Lett. **52**, 530 (1990).

Translated by R. Tyapaev

Publisher's Note. Pleiades Publishing remains neutral with regard to jurisdictional claims in published maps and institutional affiliations.